nature neuroscience

BRIEF COMMUNICATION

https://doi.org/10.1038/s41593-018-0156-7

# mTORC2, but not mTORC1, is required for hippocampal mGluR-LTD and associated behaviors

Ping Jun Zhu[1,2,3], Chien-Ju Chen[1,2,3], Jacqunae Mays[1,2], Loredana Stoica[1,2] and Mauro Costa-Mattioli[1,2*]

**The mechanistic target of rapamycin complex 1 (mTORC1) has been reported to be necessary for metabotropic glutamate receptor-mediated long-term depression (mGluR-LTD). Here we found that mTORC1-deficient mice exhibit normal hippocampal mGluR-LTD and associated behaviors. Moreover, rapamycin blocks mGluR-LTD in mTORC1-deficient mice. However, both rapamycin and mGluR activation regulate mTOR complex 2 (mTORC2) activity, and mTORC2-deficient mice show impaired mGluR-LTD and associated behaviors. Thus, mTORC2 is a major regulator of mGluR-LTD.**

Activation of group I metabotropic glutamate receptors (mGluRs) at hippocampal CA1 synapses induces a form of long-term depression (LTD) that depends on the synthesis of new proteins[1]. mGluR-LTD is altered in a variety of neurological disorders[1]. Thus, understanding the molecular mechanisms underlying mGluR-LTD is crucial because it could lead to the potential development of new treatments for mGluR-LTD-associated cognitive disorders[1].

The mechanistic target of rapamycin (mTOR) complex 1 (mTORC1) is a highly conserved signaling hub integrating a

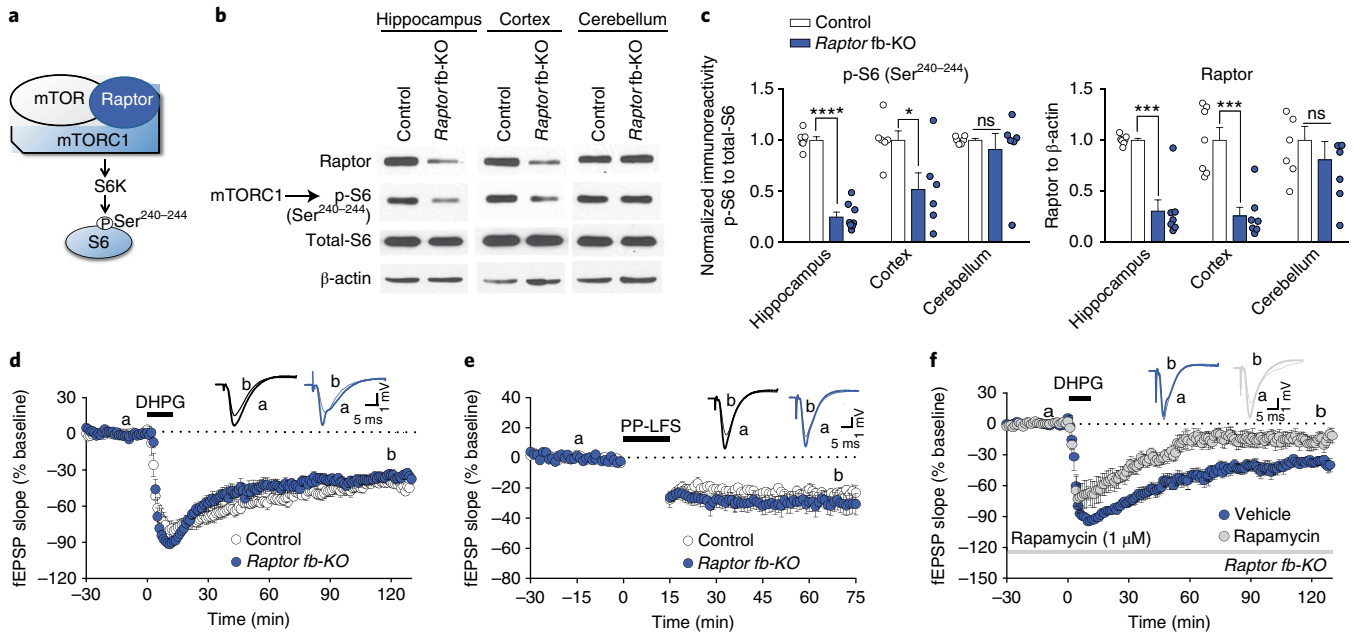


**Fig. 1 | Hippocampal mGluR-LTD is normal in mTORC1-deficient mice, but is sensitive to rapamycin. a**, Schematic of mTORC1. **b**,**c**, Representative western blots (**b**) and quantification (**c**) show reduced Raptor levels and mTORC1 activity (p-S6) in hippocampus and cortex, but not cerebellum, of *Raptor* fb-KO mice (p-S6-Ser$^{240–244}$: hippocampus control $n=7$, *Raptor* fb-KO $n=8$, $t_{13}=13.53$, $P<0.0001$; cortex control $n=6$, *Raptor* fb-KO $n=6$, $t_{10}=2.69$, $P<0.0244$, cerebellum control $n=6$, *Raptor* fb-KO $n=6$, $t_{10}=0.58$, $P=0.57$; Raptor: hippocampus control $n=7$, *Raptor* fb-KO $n=7$, $t_{12}=6.72$, $P<0.001$, cortex control $n=7$, *Raptor* fb-KO $n=7$, $t_{12}=5.03$, $P<0.001$, cerebellum control $n=6$, *Raptor* fb-KO $n=6$, $t_{10}=0.58$, $P=0.59$). fEPSPs, field excitatory postsynaptic potentials. **d**,**e**, LTD induced either with (**d**) DHPG (100 μM, 10 min; control $n=12$, *Raptor* fb-KO mice $n=8$, LTD magnitude during last 10 min: control = −43.1 ± 2.4; *Raptor* fb-KO mice = −37.9 ± 3.7, $t_{18}=1.354$, $P=0.193$) or (**e**) paired-pulse stimulation at low frequency (PP-LFS; pairs of pulses, 50-ms interval, delivered at 1 Hz, 900 pulses; control $n=7$, *Raptor* fb-KO mice $n=12$, LTD magnitude during last 10 min: control = −25.1 ± 4.5; *Raptor* fb-KO mice = −32.1 ± 3.4, $t_{17}=1.354$, $P=0.583$) is intact in *Raptor* fb-KO mice. **f**, DHPG-induced LTD in *Raptor* fb-KO is sensitive to rapamycin (1 μM; vehicle $n=8$; rapamycin $n=7$; LTD magnitude during last 10 min: vehicle = −35.1 ± 3.8; rapamycin = −17.9 ± 5.9, Mann–Whitney rank-sum test, $U=5.0$, $P<0.01$). Horizontal bars indicate periods of drug application or synaptic stimulation. Inset: superimposed traces obtained before (a) and after (b) stimulation. All data are presented as mean ± s.e.m. Statistics were based on two-sided Student's *t* test unless otherwise specified; ns, not significant. Images of western blots were cropped to show only representative figures. Full-length blots can be found in Supplementary Fig. 8.

[1]Department of Neuroscience, Baylor College of Medicine, Houston, TX, USA. [2]Memory and Brain Research Center, Baylor College of Medicine, Houston, TX, USA. [3]These authors contributed equally: Ping Jun Zhu, Chien-Ju Chen. *e-mail: costamat@bcm.edu

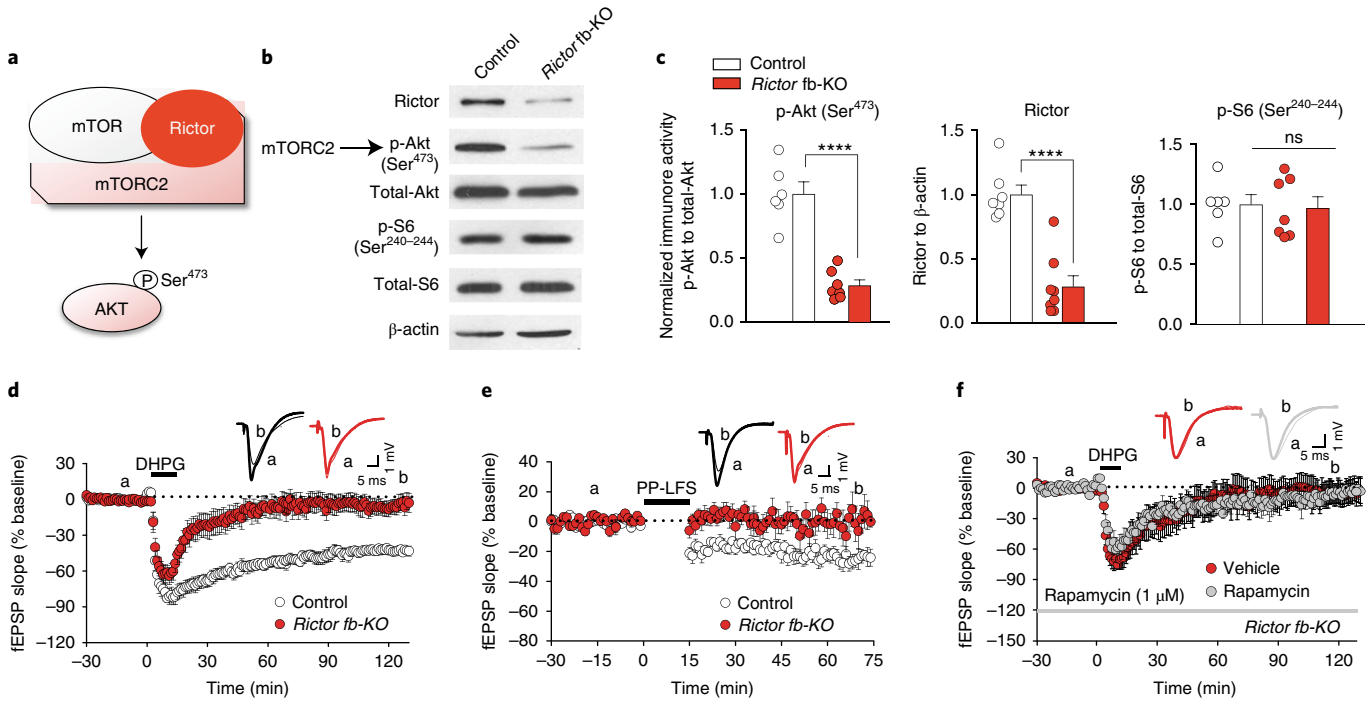


**Fig. 2 | Hippocampal mGluR-LTD is impaired in mTORC2-deficient mice. a**, Schematic of mTORC2. **b**,**c**, Representative western blots (**b**) and quantification (**c**) show reduced Rictor levels and mTORC2 activity (p-Akt-Ser$^{473}$), but not mTORC1 activity (p-S6-Ser$^{240-244}$), in the hippocampus of *Rictor* fb-KO mice (p-Akt-Ser$^{473}$: control $n=6$, *Rictor* fb-KO $n=7$, $t_{11}=7.27$, $P<0.0001$; Rictor: control $n=7$, *Rictor* fb-KO $n=8$, $t_{13}=6.31$, $P<0.0001$; p-S6-Ser$^{240-244}$: control $n=6$, *Rictor* fb-KO $n=7$: $t_{11}=0.23$, $P=0.82$). **d**,**e**, LTD induced either with (**d**) DHPG (100 μM, 10 min; control $n=10$; *Rictor* fb-KO mice $n=12$, LTD magnitude during last 10 min: control = −44.3 ± 2.5; *Rictor* fb-KO mice = −9.1 ± 5.9, $t_{20}=6.113$, $P<0.001$) or (**e**) PP-LFS (pairs of pulses, 50-ms interval, delivered at 1 Hz, 900 pulses; control $n=9$; *Rictor* fb-KO mice $n=8$, LTD magnitude during last 10 min: control = −25.7 ± 4.3; *Rictor* fb-KO mice = 2.5 ± 8.7, $t_{15}=2.989$, $P=0.009$) is impaired in *Rictor* fb-KO mice. **f**, DHPG-induced LTD in *Rictor* fb-KO mice is not further reduced by rapamycin (1 μM; vehicle $n=7$, rapamycin $n=6$, LTD magnitude during last 10 min: vehicle = −7.2 ± 2.7; rapamycin = −5.9 ± 8.1, $t_{11}=0.128$, $P=0.91$). Inset: superimposed traces obtained before (a) and after (b) stimulation. All data are presented as mean ± s.e.m. The statistics were based on two-sided Student's *t* test; ns, not significant. Images of western blots were cropped to show only representative figures. Full-length blots can be found in Supplementary Fig. 8.

variety of synaptic inputs and is a major regulator of protein synthesis rates in neurons[2,3]. The importance of mTORC1 signaling in brain processes is underscored by its postulated function in long-lasting forms of synaptic plasticity and the many neurological disorders in which mTORC1 activity is perturbed[2,3]. Indeed, mTORC1 has been reported to be necessary for hippocampal mGluR-LTD[1,4]. However, most of the evidence supporting the role of mTORC1 in mGluR-LTD is based on its pharmacological inhibition with the drug rapamycin, but recent results have challenged these findings[5].

To further investigate the role of mTORC1 in mGluR-LTD, we used molecular genetics and conditionally deleted *Raptor* (which encodes the regulatory-associated protein of mTOR, a defining component of mTORC1; Fig. 1a)[6,7] in the murine forebrain by crossing *loxP*-flanked *Raptor* mice with CaMKIIα-Cre mice, thus generating mTORC1-deficient mice (see Methods). As expected, in the hippocampus and cortex of *Raptor* forebrain knockout (*Raptor* fb-KO) mice, Raptor levels and mTORC1 activity—as determined by phosphorylation of its downstream target, ribosomal S6 (p-S6)—were significantly reduced compared to control littermates (Fig. 1b,c). Accordingly, immunohistochemistry did not detect mTORC1 activity at CA1 neurons from *Raptor* fb-KO mice (Supplementary Fig. 1). However, in the cerebellum, where Cre is expressed only modestly, mTORC1 activity and Raptor levels remained unaltered (Fig. 1b,c). Thus, deletion of *Raptor* selectively reduced mTORC1 activity in the forebrain.

To investigate the role of mTORC1 in mGluR-LTD, hippocampal slices from control and *Raptor* fb-KO mice were treated with the selective mGluR1- and mGluR5-agonist DHPG (R,S-dihydroxyphenylglycine; 100 μM, 10 min), which is known to reliably induce mGluR-LTD at CA1 synapses[8]. Unexpectedly, we found that DPHG resulted in normal depression of field excitatory postsynaptic potentials at Schaffer collateral-CA1 neurons in *Raptor* fb-KO slices, with a magnitude and time course similar to that of control littermates (Fig. 1d). Accordingly, paired-pulse stimulation at low frequency elicited similar mGluR-LTDs of synaptic transmission in both control and *Raptor* fb-KO slices (Fig. 1e). It is noteworthy that basal synaptic transmission was normal in hippocampal slices from *Raptor* fb-KO and control littermates, as determined by analysis of paired-pulse facilitation and input–output relationships (Supplementary Fig. 2). Thus, irrespective of the mGluR-LTD-inducing protocol, conditional deletion of mTORC1 in CA1 neurons had no effect on mGluR-induced LTD.

Given the conflicting results regarding the effects of rapamycin on mGluR-LTD[4,5], we treated hippocampal slices from wild-type control mice with different concentrations of rapamycin. Notably, mGluR-LTD was insensitive to treatment with low concentrations of rapamycin (20 nM and 200 nM; Supplementary Fig. 3a,b). By contrast, a high concentration of rapamycin (1 μM) prevented mGluR-LTD in control slices (Supplementary Fig. 3c), but had no effect on basal synaptic properties (Supplementary Fig. 4). All concentrations of rapamycin reduced mTORC1 activity (Supplementary Fig. 3d,e), suggesting that the high concentration of rapamycin (1 μM) may block mGluR-LTD in an mTORC1-independent manner. To directly test this possibility, we examined the effect of a high concentration of rapamycin (1 μM) on mGluR-LTD in hippocampal slices from mTORC1-deficient mice. Since rapamycin is reported

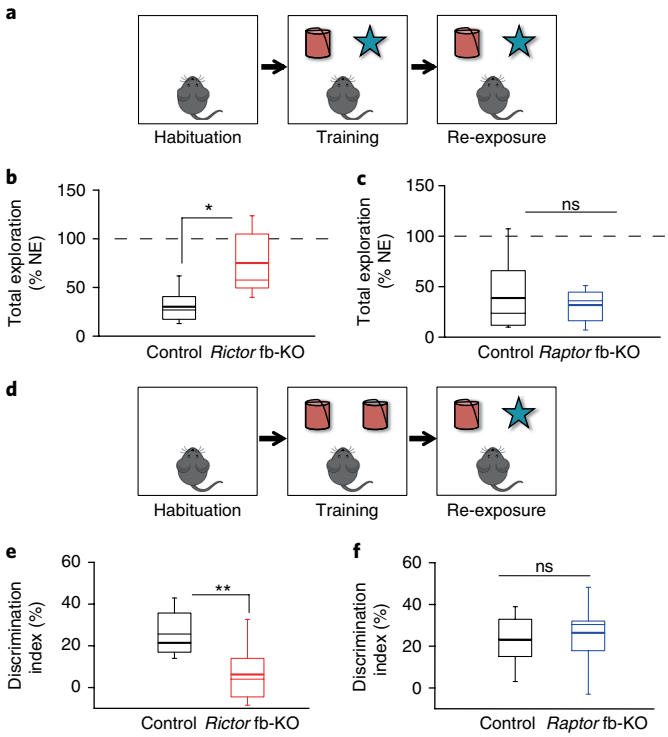


**Fig. 3 | mTORC2, but not mTORC1, is required for hippocampal-mediated mGluR-LTD related behavior. a**, Experimental model of the spatial recognition task. After habituating in an empty box, mice are exposed to two novel objects on the following day (training), and then re-exposed to the same objects 24 h later (re-exposure). **b**, During re-exposure, *Rictor* fb-KO mice ($n=10$) spent more time exploring the objects than control littermates ($n=13$; Mann–Whitney rank-sum test, $U=13.0$, $P<0.001$). NE, novel exploration. **c**, Hippocampal-dependent spatial recognition is intact in *Raptor* fb-KO mice ($n=8$), as they spend similar times as control littermates ($n=10$) exploring the objects during re-exposure (Mann–Whitney rank-sum test, $U=61$, $P=0.828$). **d**, Experimental design for the object recognition task. **e**, *Rictor* fb-KO mice ($n=11$) show significantly lower preference for novel objects than control littermates ($n=12$; Mann–Whitney rank-sum test, $U=18$, $P<0.001$). **f**, Object recognition is intact in *Raptor* fb-KO mice ($n=11$), as they spend similar times as control littermates ($n=12$) exploring novel objects during re-exposure (two-sided Student's *t* test, $t_{21}=0.613$, $P=0.547$). Box plots show the minimum, maximum, median, and 25th and 75th percentiles of the groups. Mean values are indicated by thick lines.

to be highly specific for mTORC1[9], it was expected to have no effect on mGluR-LTD in *Raptor* fb-KO mice. However, as in control slices (Supplementary Fig. 3c), rapamycin (1 μM) inhibited mGluR-LTD in *Raptor* fb-KO slices (Fig. 1f). Hence, these data support the notion that the effects of rapamycin on mGluR-LTD at CA1 synapses are independent of mTORC1.

In addition to mTORC1, another structurally and functionally distinct mTOR-containing complex, mTORC2, has been identified more recently[6,7]. While little is known regarding its upstream regulation and downstream effectors, mTORC2 contains Rictor (rapamycin-insensitive companion of mTOR; Fig. 2a) as an essential component that is largely insensitive to acute rapamycin treatment[6,7]. However, in cancer cells, prolonged rapamycin treatment[10] or higher concentrations of rapamycin[11] suppress mTORC2 activity. Could mTORC2, but not mTORC1, be the major regulator of mGluR-LTD in the mammalian brain? We began addressing this question by examining whether mGluR activation engages mTORC2 function. We found that treatment with DHPG (100 μM, 10 min) increased the activity of mTORC2, as determined by the phosphorylation of its downstream target Akt at Ser-473, a reliable readout of mTORC2 activity[6,7] (Supplementary Fig. 5a,b).

We next asked whether the high concentration of rapamycin (1 μM) sufficient to suppress mGluR-LTD would also block mTORC2 activity in control slices. Indeed, we found that high (1 μM), but not low (20 nM and 200 nM), concentrations of rapamycin reduced mTORC2 activity (Supplementary Fig. 5c,d). To investigate whether mTORC2 is required for mGluR-LTD at CA1 synapses, we studied mTORC2-deficient mice, in which *Rictor* (which encodes mTORC2's defining component) was conditionally deleted in the murine forebrain postnatally (*Rictor* fb-KO mice)[12]. As we have previously shown, mTORC2 activity is selectively reduced in the hippocampus from *Rictor* fb-KO mice (Fig. 2b,c), and basal synaptic transmission is not altered in these mice[12]. As expected, DHPG induced a typical LTD of field excitatory postsynaptic potentials in control slices (Fig. 2d). However, in *Rictor* fb-KO slices, the same stimulation protocol failed to elicit mGluR-LTD (Fig. 2d). In agreement with these observations, synaptic induction of mGluR-LTD with paired-pulse stimulation at low frequency was also impaired in *Rictor* fb-KO slices (Fig. 2e). Moreover, a high concentration of rapamycin (1 μM) did not further reduce mGluR-LTD in *Rictor* fb-KO slices (Fig. 2f). Taken together, our results indicate that mTORC2, but not mTORC1, is required for mGluR-LTD at CA1 synapses.

mGluR-LTD contributes to different types of hippocampal learning and memory processes. Specifically, spatial recognition of objects has been reported to trigger a long-lasting hippocampal LTD at Schaffer collateral CA1 synapses in freely moving animals (during training; Fig. 3a)[13,14]. Re-exposure to the same objects on the following day is associated with reduced exploration time and absence of LTD in vivo[13,14]. Inhibition of mGluR receptors immediately before exposure to novel objects (training) blocks LTD and the concomitant reduction in re-exploration during re-exposure[14], indicating that this in vivo LTD depends, at least in part, on mGluR receptors. Because mGluR-LTD is impaired in slices from mTORC2-deficient mice, we next examined whether spatial recognition is also deficient in these mice. Indeed, *Rictor* fb-KO mice spent more time exploring the same objects compared to control littermates (Fig. 3b), indicating that mTORC2 is required for learning mediated by hippocampal mGluR-LTD. Accordingly, mTORC2-deficient mice were also impaired in novel object recognition (Fig. 3e), another hippocampal LTD-inducing task[14] (Fig. 3d). The impaired hippocampal mGluR-LTD-mediated behavior in mTORC2-deficient mice is not caused by nonspecific exploratory responses, because distance traveled and exploratory behavior were similar between control and *Rictor* fb-KO mice (Supplementary Fig. 6a,b).

Because mGluR-LTD was not altered in mTORC1-deficient mice, we predicted that mGluR-LTD-related behaviors should be normal in these mice. Consistent with this prediction, we found that both spatial recognition (Fig. 3c) and object recognition (Fig. 3f) were normal in *Raptor* fb-KO mice, indicating that hippocampal mGluR-LTD and correlated behaviors did not depend on mTORC1. Finally, chronic rapamycin treatment, inhibiting both mTORC1 and mTORC2[15], blocked spatial and object recognition (Supplementary Fig. 7). Thus, rapamycin-treated mice resemble *Rictor* fb-KO mice but not *Raptor* fb-KO mice with respect to their requirement for mGluR-LTD associated behaviors. Taken together, these data indicate that mTORC2, but not mTORC1, is required for hippocampal mGluR-LTD and associated behaviors.

mGluR-LTD is dependent on new protein synthesis[16]. While mTORC1 is a major regulator of protein synthesis in the brain[2,3], our results suggest that the translational program underlying mGluR-LTD at CA1 synapses is independent of mTORC1. Regulation of protein synthesis at the levels of (i) initiation, by the translation initiation factor eIF2α[17], or (ii) elongation[18], might better explain

this protein synthesis-dependent form of synaptic plasticity. While not required for hippocampal mGluR-LTD, mTORC1 is necessary for hippocampal long-term potentiation (late-LTP), another major form of synaptic plasticity in the mammalian brain, and related behaviors[19] (but also see ref. [20]). Thus, we propose that mTORC1 at CA1 synapses is selectively required for protein synthesis-dependent increases (late-LTP), but not decreases (LTD), in synaptic efficacy.

Finally, mGluR-LTD is altered in a variety of neurological disorders, including autism spectrum disorders, intellectual disability, Alzheimer's disease, epilepsy, and drug addiction[1]. In the last few years, study of the molecular mechanisms implicated in mGluR-LTD has led to the development of 'mechanism-based treatments' for some of these disorders. Unexpectedly, our results support the notion that mTORC2, but not mTORC1, is the major mTOR complex driving mGluR-LTD in the adult mammalian brain. Thus, modulation of mTORC2 may emerge as a promising new avenue for the treatment of mGluR-LTD-related disorders.

## Methods

Methods, including statements of data availability and any associated accession codes and references, are available at https://doi.org/10.1038/s41593-018-0156-7.

Received: 3 October 2017; Accepted: 19 April 2018;
Published online: 21 May 2018

## References

1. Lüscher, C. & Huber, K. M. *Neuron* **65**, 445–459 (2010).
2. Costa-Mattioli, M. & Monteggia, L. M. *Nat. Neurosci.* **16**, 1537–1543 (2013).
3. Hoeffer, C. A. & Klann, E. *Trends Neurosci.* **33**, 67–75 (2010).
4. Hou, L. & Klann, E. *J. Neurosci.* **24**, 6352–6361 (2004).
5. Auerbach, B. D., Osterweil, E. K. & Bear, M. F. *Nature* **480**, 63–68 (2011).
6. Laplante, M. & Sabatini, D. M. *Cell* **149**, 274–293 (2012).
7. Wullschleger, S., Loewith, R. & Hall, M. N. *Cell* **124**, 471–484 (2006).
8. Palmer, M. J., Irving, A. J., Seabrook, G. R., Jane, D. E. & Collingridge, G. L. *Neuropharmacology* **36**, 1517–1532 (1997).
9. Benjamin, D., Colombi, M., Moroni, C. & Hall, M. N. *Nat. Rev. Drug Discov.* **10**, 868–880 (2011).
10. Sarbassov, D. D. et al. *Mol. Cell* **22**, 159–168 (2006).
11. Toschi, A. et al. *Mol. Cell. Biol.* **29**, 1411–1420 (2009).
12. Huang, W. et al. *Nat. Neurosci.* **16**, 441–448 (2013).
13. Goh, J. J. & Manahan-Vaughan, D. *Cereb. Cortex* **23**, 1118–1125 (2013).
14. Goh, J. J. & Manahan-Vaughan, D. *Hippocampus* **23**, 129–138 (2013).
15. Lamming, D. W. et al. *Science* **335**, 1638–1643 (2012).
16. Huber, K. M., Kayser, M. S. & Bear, M. F. *Science* **288**, 1254–1257 (2000).
17. Di Prisco, G. V. et al. *Nat. Neurosci.* **17**, 1073–1082 (2014).
18. Graber, T. E. et al. *Proc. Natl. Acad. Sci. USA* **110**, 16205–16210 (2013).
19. Stoica, L. et al. *Proc. Natl. Acad. Sci. USA* **108**, 3791–3796 (2011).
20. Goorden, S. M. et al. *Hum. Mol. Genet.* **24**, 3390–3398 (2015).

## Acknowledgements

We thank K. Krnjevic, A. Placzek, and members of the Costa-Mattioli lab for comments on the manuscript. This work was supported by funds to M.C.-M. (NIMH 096816 and 112356, NINDS 076708, Department of Defense AR120254, Sammons Enterprises).

## Author contributions

P.J.Z., C.-J.C., J.M., and M.C.-M. designed the experiments and wrote the manuscript; P.J.Z. conducted electrophysiology, behavioral, and immunoblotting experiments and analyzed data. C.-J.C performed behavioral, immunohistochemistry, and immunoblotting experiments and analyzed data. J.M. conducted immunoblotting experiments and analyzed data. L.S. performed immunoblotting experiments and analyzed data.

## Competing interests

The authors declare no competing interests.

## Additional information

**Supplementary information** is available for this paper at https://doi.org/10.1038/s41593-018-0156-7.

**Reprints and permissions information** is available at www.nature.com/reprints.

**Correspondence and requests for materials** should be addressed to M.C.

**Publisher's note:** Springer Nature remains neutral with regard to jurisdictional claims in published maps and institutional affiliations.

## Methods

**Mouse husbandry.** All experiments were conducted on 3- to 6-month old male and female mice on a C57Bl/6 background. *Raptor*$^{loxP/loxP}$ mice were purchased from Jackson laboratory (Stock #013188) and crossed with mice expressing *Cre* recombinase under the control of the α subunit of calcium/calmodulin-dependent protein kinase II (*Camk2α*) promoter (*Camk2α-Cre*)[21,22], thus generating *Raptor* fb-KO mice. Mice were weaned at the third postnatal week and genotyped by PCR. Raptor mutant and wild-type alleles were detected by PCR assay in which primer F11117 (5′-CTCAGTAGTGGTATGTGCTCA-3′) and primer R11118 (5′-GGGTACAGTATGTCAGCACAG-3′) amplify a 141-basepair fragment (wild-type) and a 180-basepair fragment (exon 6 of the *Raptor* conditional allele). Cre expression was detected by PCR with primers CreF3 (5′-GGCCCAGCTTTCTCATATTTG-3′) and CreR3 (5′-TCAGCTACACCAGAGACG-3′), which amplify a 488-basepair fragment. *Rictor* fb-KO mice were previously described[12]. Mice were kept on a 12-h/12-h light/dark cycle (lights on at 7:00 a.m.) and had access to food and water ad libitum. Animal care and experimental procedures were approved by the institutional animal care and use committee (IACUC) at Baylor College of Medicine, according to NIH guidelines.

**Slice electrophysiology.** Electrophysiological recordings were performed, as previously described[12,23]. The investigators were blind to mouse genotypes. Briefly, horizontal hippocampal slices (320 µm thick) were cut with a vibratome (Leica VT 1000 S, Leica Microsystems, Buffalo Grove, IL) at 4 °C in artificial cerebrospinal fluid solution (ACSF; 95% $O_2$ and 5% $CO_2$) containing, in mM: 124 NaCl, 2.0 KCl, 1.3 $MgSO_4$, 2.5 $CaCl_2$, 1.2 $KH_2PO_4$, 25 $NaHCO_3$, and 10 glucose (2–3 mL/min). Slices were incubated for at least 60 min before recording in an interface chamber and continuously perfused with artificial cerebrospinal fluid (ACSF) at 30 °C and a flow rate of 2–3 mL/min. The recording electrodes were placed in the stratum radiatum. Field excitatory postsynaptic potentials (fEPSPs) were recorded with ACSF-filled micropipettes and were elicited by bipolar stimulating electrodes placed in the CA1 stratum radiatum to excite Schaffer collateral and commissural fibers. The intensity of the 0.1-ms pulses was adjusted to evoke 40–50% of maximal response. A stable baseline of responses at 0.033 Hz was established for at least 30 min. mGluR-LTD was induced by bath-application of DHPG (100 µM) for 10 min or by pairing stimuli (interstimulus interval, 50 ms) delivered at 1 Hz for 15 min (900 pulses; PP-LFS), as previously described[24]. For the experiments with rapamycin, hippocampal slices were preincubated in the recording chamber with rapamycin (20 nM, 200 nM, or 1 µM) for 30 min before DHPG application, and rapamycin was kept throughout the recording. All data are presented as means ± s.e.m. and *n* refers to both the number of slices and the number of mice, as appropriate. All drugs were obtained from Tocris (Ellisville, MO).

**Western blotting.** The hippocampus, cortex, and cerebellum from control and *Raptor* fb-KO mice were isolated, homogenized in cold homogenizing buffer (200 mM HEPES, 50 mM NaCl, 10% glycerol, 1% Triton X-100, 1 mM EDTA, 50 mM NaF, 2 mM $Na_3VO_4$, 25 mM β-glycerophosphate, and EDTA-free complete ULTRA tablets (Roche, Indianapolis, IN), and centrifuged at 13,000 *g* for 10 min. The supernatants (of 30 µg of protein/sample) were resolved on SDS–PAGE (10%) and transferred onto nitrocellulose membranes (Pall, Port Washington, NY). Treatment with DHPG, followed by biochemical analysis, was performed as previously described[4]. Briefly, after treatments, slices were snap-frozen on dry ice, then suspended in lysis buffer and analyzed by western blotting, which was performed as we previously described[12,19]. Antibodies against p-S6 (1:1,000, $Ser^{240-244}$ #5364), p-Akt (1:1,000, $Ser^{473}$ #9271), total S6 (1:1,000 #2217), total Akt (1:1,000 #9272), Raptor (1:1,000 #2280), and Rictor (1:1,000 #2114) were purchased from Cell Signaling and Technology Laboratories (Danvers, MA); β-actin (1:5,000 #1501) was purchased from Millipore (Temecula, CA).

**Spatial and object recognition.** The investigators performing and scoring the behavior were blind to genotype and treatment. Spatial and object recognition were performed as previously described[13,14,17], with only slight modifications. For all behavioral experiments, we included similar numbers of male and female mice for each genotype. No differences were between males and females were found (data not shown). Mice were handled for 5–10 min and habituated ('habituation') to a black Plexiglas rectangular chamber (31 × 24 cm, height 27 cm) for 10 min under dim ambient light for 3 d. Exploration of the objects was defined as sniffing of the objects (with nose contact or head directed toward the object) within a 2-cm radius of the objects. Sitting or standing on the objects was not scored as exploration. Behavior was recorded from cameras positioned above the training chamber. Data are expressed as a percentage of re-exploration ('re-exposure') relative to the initial exploration time (during 'training').

For novel-object recognition training, two identical objects were presented to mice to explore for 5 min, after which mice were returned to the home cage. Twenty-four hours later, one object was replaced by one novel object and the mouse was again placed in the chamber 5 min. The novel object had the same height and volume as the object it replaced, but different shape and appearance. The discrimination index (DI) was computed as DI = (novel-object exploration time – familiar-object exploration time/total exploration time) × 100. To control for odor cues, the open field arena and the objects were thoroughly cleaned with ethanol, dried, and ventilated between mice.

**Immunofluorescence.** Mice were anesthetized by isoflurane and perfused transcardially with cold 0.9% phosphate-buffered saline (PBS), followed by 4% paraformaldehyde in PBS. Brain samples were then postfixed in 4% paraformaldehyde at 4 °C overnight and cryoprotected in 30% sucrose in BPS for 3 days. Free-floating frozen sagittal sections (25 µm) were incubated in blocking solution (10% normal goat serum, 0.3% Triton X-100, 0.01% sodium azide in PBS) for 1 h at room temperature (23–25 °C) and then transferred into diluted primary antibodies (mouse anti-NeuN, Abcam #104224, 1:500; rabbit anti-pS6-$Ser^{240/244}$, Cell Signaling Technology #5364, 1:300) for incubation overnight. Primary antibodies were visualized using florescence-conjugated antibodies (1:1,000, goat anti-rabbit Alexa Fluor 488, ThermoFisher Scientific, #A-11034; goat anti-mouse Alexa Fluor 594, ThermoFisher Scientific, #A-11032). Image acquisition and processing were performed as we previously described[25].

**Rapamycin administration.** Mice received intraperitoneal (i.p) injections of rapamycin (10 mg/kg, LC Laboratories, Woburn MA) or vehicle (4% ethanol, 4% Tween-80, and 4% PEG-400) daily for 6 days before behavioral tests.

**Statistical analyses.** No statistical methods were used to predetermine sample sizes, but our sample sizes are selected based on previous studies published in the field (see Reporting Summary for references). Animals in the same litter were randomly assigned to different treatment groups in various experiments. No animals or data points were excluded from the analysis. Normality tests and *F* tests for equality of variances were performed before choosing the statistical test. Statistics were based on two-sided Student's *t* tests or Mann–Whitney rank-sum tests for two-group comparisons (for datasets that were not normally distributed). One-way ANOVA followed by Bonferroni post hoc analyses were performed for multiple comparisons, unless otherwise indicated. $P < 0.05$ was considered significant ($^*P < 0.05$, $^{**}P < 0.01$, $^{***}P < 0.001$).

**Reporting Summary.** Further information on experimental design is available in the Nature Research Reporting Summary linked to this article.

**Data availability.** The data that support the findings of this study are available from the corresponding author upon reasonable request.

## References

21. Dragatsis, I. & Zeitlin, S. *Genesis.* **26**, 133–135 (2000).
22. Tsien, J. Z. et al. *Cell* **87**, 1317–1326 (1996).
23. Zhu, P. J. et al. *Cell* **147**, 1384–1396 (2011).
24. Ronesi, J. A. & Huber, K. M. *J. Neurosci.* **28**, 543–547 (2008).
25. Buffington, S. A. et al. *Cell* **165**, 1762–1775 (2016).

nature research

Corresponding author(s): NN-BC61875C

# Reporting Summary

Nature Research wishes to improve the reproducibility of the work that we publish. This form provides structure for consistency and transparency in reporting. For further information on Nature Research policies, see Authors & Referees and the Editorial Policy Checklist.

## Statistical parameters

When statistical analyses are reported, confirm that the following items are present in the relevant location (e.g. figure legend, table legend, main text, or Methods section).

| n/a | Confirmed | |
|---|---|---|
| ☐ | ☒ | The exact sample size (*n*) for each experimental group/condition, given as a discrete number and unit of measurement |
| ☐ | ☒ | An indication of whether measurements were taken from distinct samples or whether the same sample was measured repeatedly |
| ☐ | ☒ | The statistical test(s) used AND whether they are one- or two-sided<br>*Only common tests should be described solely by name; describe more complex techniques in the Methods section.* |
| ☐ | ☒ | A description of all covariates tested |
| ☐ | ☒ | A description of any assumptions or corrections, such as tests of normality and adjustment for multiple comparisons |
| ☐ | ☒ | A full description of the statistics including central tendency (e.g. means) or other basic estimates (e.g. regression coefficient) AND variation (e.g. standard deviation) or associated estimates of uncertainty (e.g. confidence intervals) |
| ☐ | ☒ | For null hypothesis testing, the test statistic (e.g. *F*, *t*, *r*) with confidence intervals, effect sizes, degrees of freedom and *P* value noted<br>*Give P values as exact values whenever suitable.* |
| ☒ | ☐ | For Bayesian analysis, information on the choice of priors and Markov chain Monte Carlo settings |
| ☒ | ☐ | For hierarchical and complex designs, identification of the appropriate level for tests and full reporting of outcomes |
| ☒ | ☐ | Estimates of effect sizes (e.g. Cohen's *d*, Pearson's *r*), indicating how they were calculated |
| ☐ | ☒ | Clearly defined error bars<br>*State explicitly what error bars represent (e.g. SD, SE, CI)* |

*Our web collection on statistics for biologists may be useful.*

## Software and code

Policy information about availability of computer code

| | |
|---|---|
| Data collection | Clampfit 10.2 (Electrophysiology), ANY-maze 4.99z (Behavior), Zen 2 Pro (Immunoflourescence) |
| Data analysis | ImageJ 1.49V(Immunoblotting), Prism7(Statistics) |

For manuscripts utilizing custom algorithms or software that are central to the research but not yet described in published literature, software must be made available to editors/reviewers upon request. We strongly encourage code deposition in a community repository (e.g. GitHub). See the Nature Research guidelines for submitting code & software for further information.

## Data

Policy information about availability of data

All manuscripts must include a data availability statement. This statement should provide the following information, where applicable:

- Accession codes, unique identifiers, or web links for publicly available datasets
- A list of figures that have associated raw data
- A description of any restrictions on data availability

The data that support the findings of this study are available from the corresponding author upon reasonable request

# Field-specific reporting

Please select the best fit for your research. If you are not sure, read the appropriate sections before making your selection.

☒ Life sciences ☐ Behavioural & social sciences

For a reference copy of the document with all sections, see nature.com/authors/policies/ReportingSummary-flat.pdf

# Life sciences

## Study design

All studies must disclose on these points even when the disclosure is negative.

| | |
|---|---|
| Sample size | No statistical methods were used to predetermine sample size. The sample size were selected based on published studies in the field (Ehnninger et al. Nat Med, 2008; Auerbach et al., Nature, 2011; Jakkamsetti et al., Neuron, 2013; Hao et al., Nature 2015; Santini et al., Nature 2013; Gkogkas et al. Nature 2013; Mathur et al., Nat Neurosci, 2013; Labouebe et al., Nat Neurosci, 2013; Atwood et al., Nature Neurosci, 2014; Knafo et al., Nat Neurosci, 2016; Uematsu et al., Nat Neurosci, 2017). |
| Data exclusions | No animals or data points were excluded from the analyses |
| Replication | All attempts at replication were successful. |
| Randomization | For molecular, behavioral and electrophysiological studies, mice were randomly assigned to control and experimental groups . |
| Blinding | These experiments were performed and analyzed blind to treatment conditions and/or genotype, information which was unveiled post-analysis. |

## Materials & experimental systems

Policy information about availability of materials

| n/a | Involved in the study |
|---|---|
| ☒ | ☐ Unique materials |
| ☐ | ☒ Antibodies |
| ☒ | ☐ Eukaryotic cell lines |
| ☐ | ☒ Research animals |
| ☒ | ☐ Human research participants |

### Antibodies

| | |
|---|---|
| Antibodies used | p-S6 (#5364, Lot 6), p-Akt (#9271, Lot 14), total S6 (#2217, Lot 7), total Akt (#9272, Lot 27), Raptor (#2280, Lot 12), and Rictor (#2114, Lot 6) were purchased from Cell Signaling Technology (Danvers, MA). β-actin (#1501, Lot 2886694) from Millipore (Temecula, CA). NeuN, (#104224, Lot GR3201902-1) from Abcam |
| Validation | All antibodies used in this study are commercially available and validated antibodies. |

### Research animals

Policy information about studies involving animals; ARRIVE guidelines recommended for reporting animal research

| | |
|---|---|
| Animals/animal-derived materials | All animals used in this study were of the species Mus musculus and the strain C57BL/6. Animals used for behavioral experiments were both males and females 3-6 months old (see Online methods). Animal care and experimental procedures were approved by the institutional animal care and use committee of Baylor College of Medicine, according to US National Institutes of Health Guidelines (Online Methods/mouse husbandry). |

# Method-specific reporting

| n/a | Involved in the study |
|---|---|
| ☒ | ☐ ChIP-seq |
| ☒ | ☐ Flow cytometry |
| ☒ | ☐ Magnetic resonance imaging |

nature neuroscience

SUPPLEMENTARY INFORMATION

https://doi.org/10.1038/s41593-018-0156-7

In the format provided by the authors and unedited.

# mTORC2, but not mTORC1, is required for hippocampal mGluR-LTD and associated behaviors

**Ping Jun Zhu[1,2,3], Chien-Ju Chen[1,2,3], Jacqunae Mays[1,2], Loredana Stoica[1,2] and Mauro Costa-Mattioli[1,2]***

[1]Department of Neuroscience, Baylor College of Medicine, Houston, TX, USA. [2]Memory and Brain Research Center, Baylor College of Medicine, Houston, TX, USA. [3]These authors contributed equally: Ping Jun Zhu, Chien-Ju Chen. *e-mail: costamat@bcm.edu

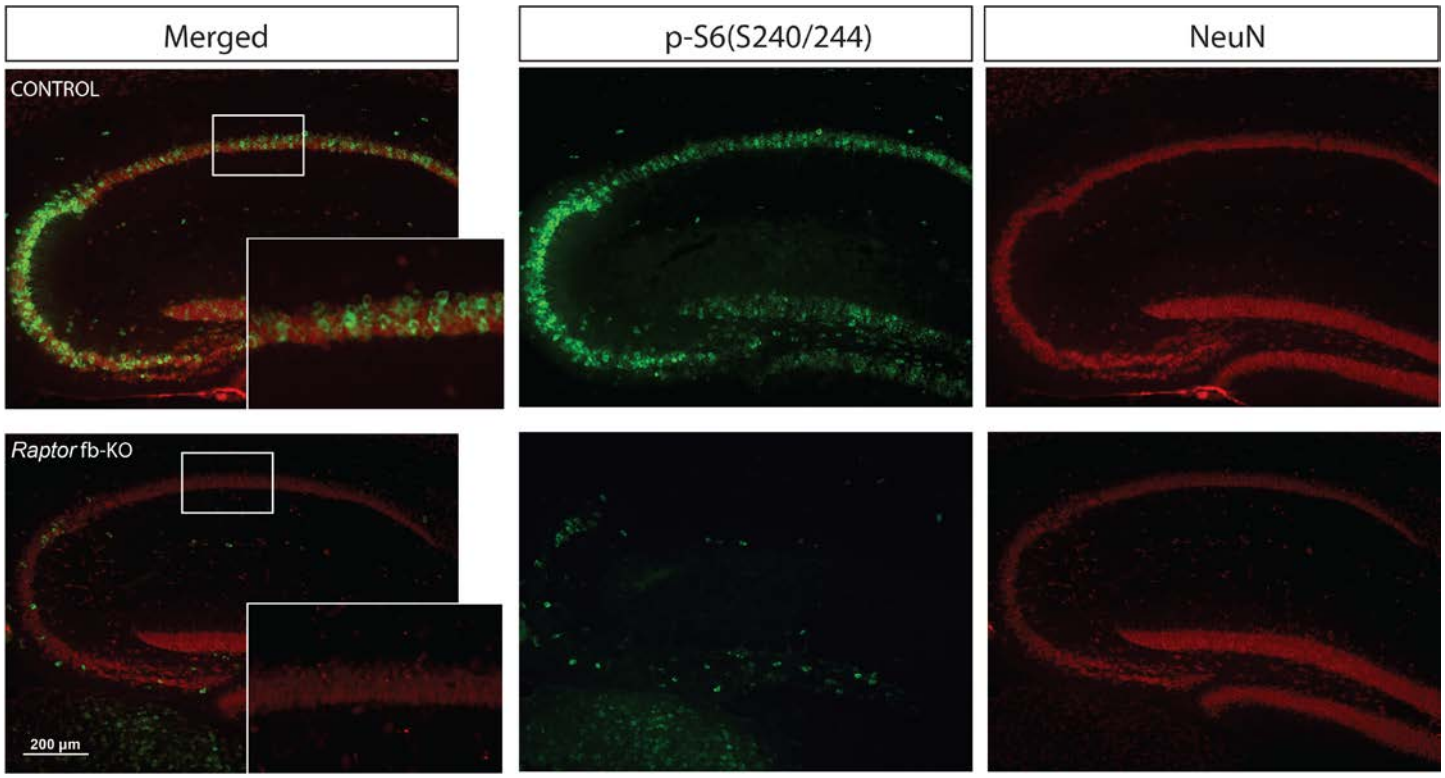


**Supplementary Figure 1**

**mTORC1 activity is undetected in hippocampal CA1 neurons of *Raptor* fb-KO mice.**

Green, immunohistochemistry staining for phosphorylated S6 (p-S6, Ser240/244). Red, immunohistochemistry staining for the neuronal marker NeuN. Experiments were repeated in two different cohorts of animals (two mice per genotype in each cohort) and samples were collected and processed separately.

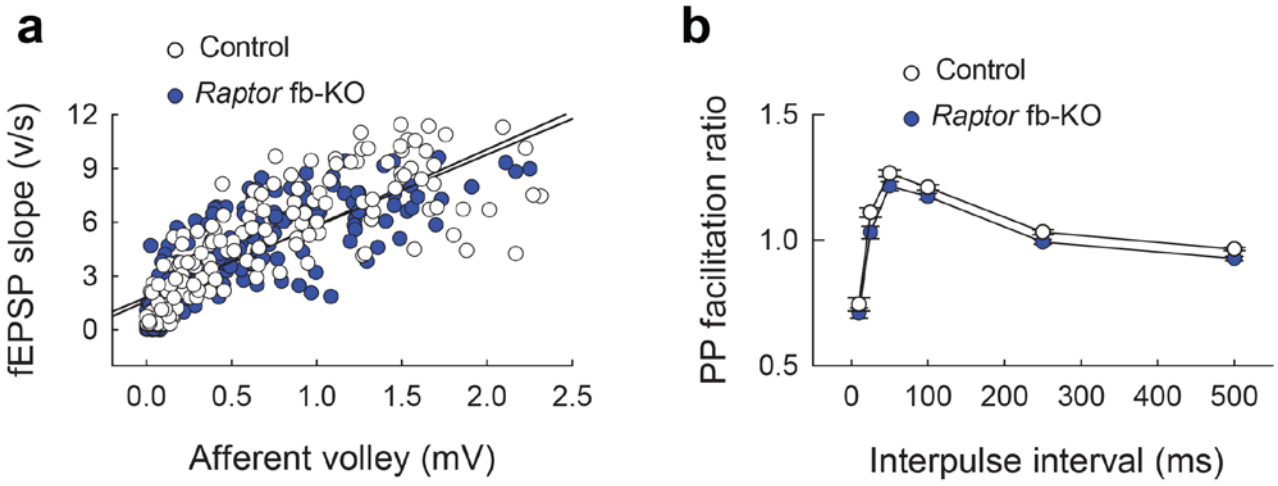


**Supplementary Figure 2**

**Basal synaptic transmission did not differ between slices from control and *Raptor* fb-KO mice.**

(**a**) Input-output plots show that fEPSPs as a function of presynaptic fiber volley was unaffected in *Raptor* fb-KO mice (n = 20) compared to control (n = 24) slices (linear regression; $R^2$ = 0.64 for control and 0.63 for Raptor fb-KO mice. (**b**) Paired-pulse (PP) facilitation did not differ between control (n = 24) and *Raptor* fb-KO mice (n = 20), as determined by the plots of PP ratio (fEPSP2/fEPSP1) for various intervals of PP stimulation.

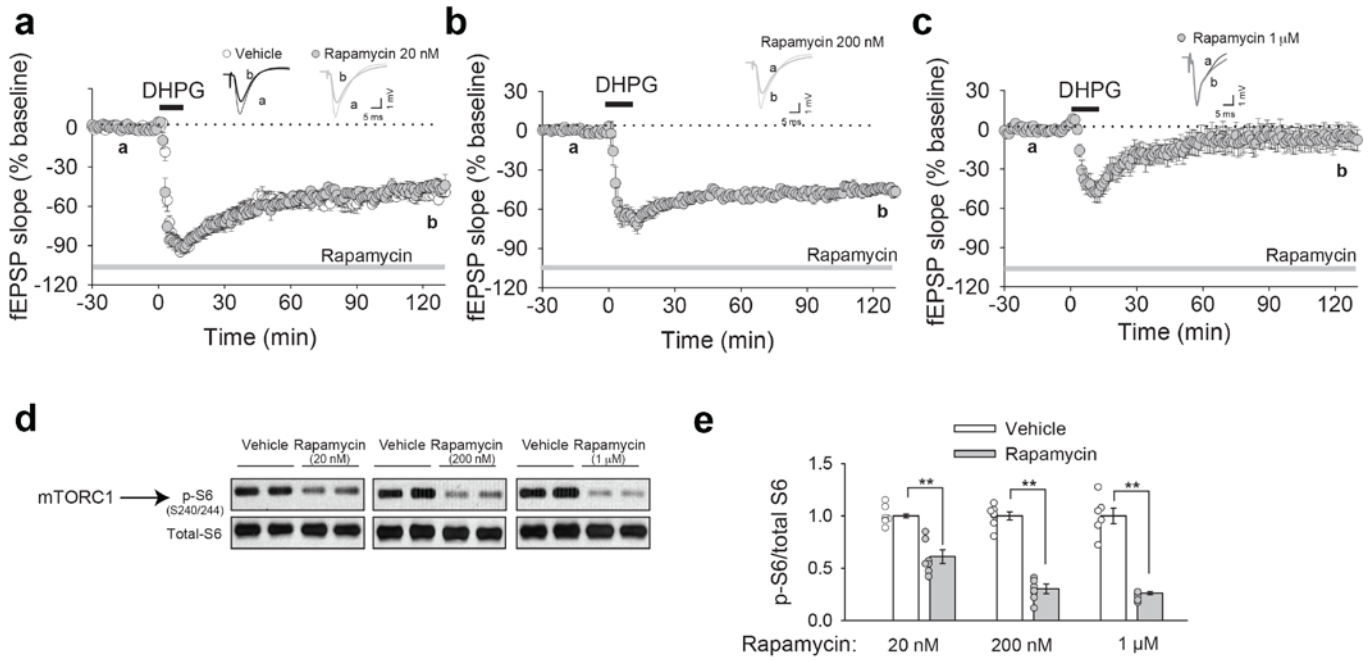


**Supplementary Figure 3**

**High, but not low, concentrations of rapamycin blocks mGluR-LTD in control slices.**

(**a-b**) Low concentrations of rapamycin (**a**, vehicle $n$ = 7, 20 nM rapamycin $n$ = 8, $t_{13}$ = 1.592, $P$ = 0.739; **b**, 200 nM rapamycin n = 8, vs vehicle $t_{13}$ = 0.289, $P$ = 1.0) had no effect on mGluR-LTD (rapamycin 20 nM vs 200 nM $t_{13}$ = 1.348, $P$ = 1.0). (**c**) mGluR-LTD is sensitive to high concentration rapamycin (1 μM rapamycin n = 8, vs vehicle $t_{13}$ = 5.102, $P$ < 0.001; rapamycin 20 nM vs rapamycin 1 μM, $t_{14}$ = 3.633, $P$ = 0.007; rapamycin 200 nM vs rapamycin 1 μM, $t_{14}$ = 4.981, $P$ < 0.001) (**d-e**) Western blot show that compared to vehicle treated slices, all concentrations of rapamycin reduce mTORC1 activity (p-S6) in control slices (20 nM rapamycin n = 7, vehicle n = 7, $t_{12}$ = 5.843, $P$ < 0.001; 200 nM rapamycin n = 7, vehicle n = 7, $t_{12}$ = 13.262, $P$ < 0.001; 1 μM rapamycin n = 6, vehicle n = 6, $t_{10}$ = 10.116, $P$ < 0.001). All data are presented as mean ± SEM. The statistics were based on two-sided Student's *t*-test. Images of western blots were cropped to show only representative samples. Full-length blots can be found in supplementary Figure 8.

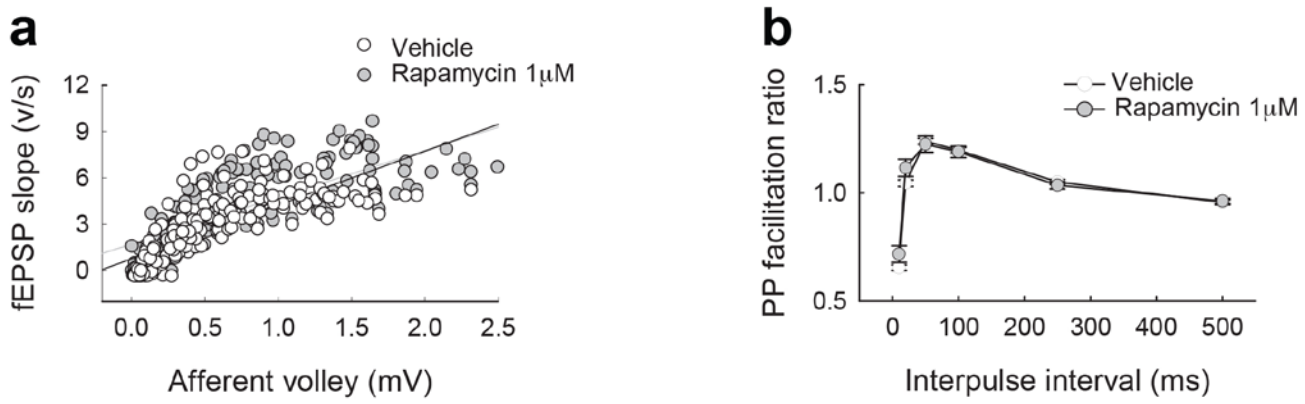


**Supplementary Figure 4**

**High concentration of rapamycin (1 μM) had no effect on basal synaptic transmission.**

Rapamycin (1 μM) did not affect fEPSPs as a function of presynaptic fiber volley (**a**), linear regression $R^2$ = 0.643 for vehicle (n=20) and 0.641 for rapamycin-treated (n=16) slice or (**b**) paired-pulse (PP) facilitation. Data points are presented as mean±SEM in (**b**).

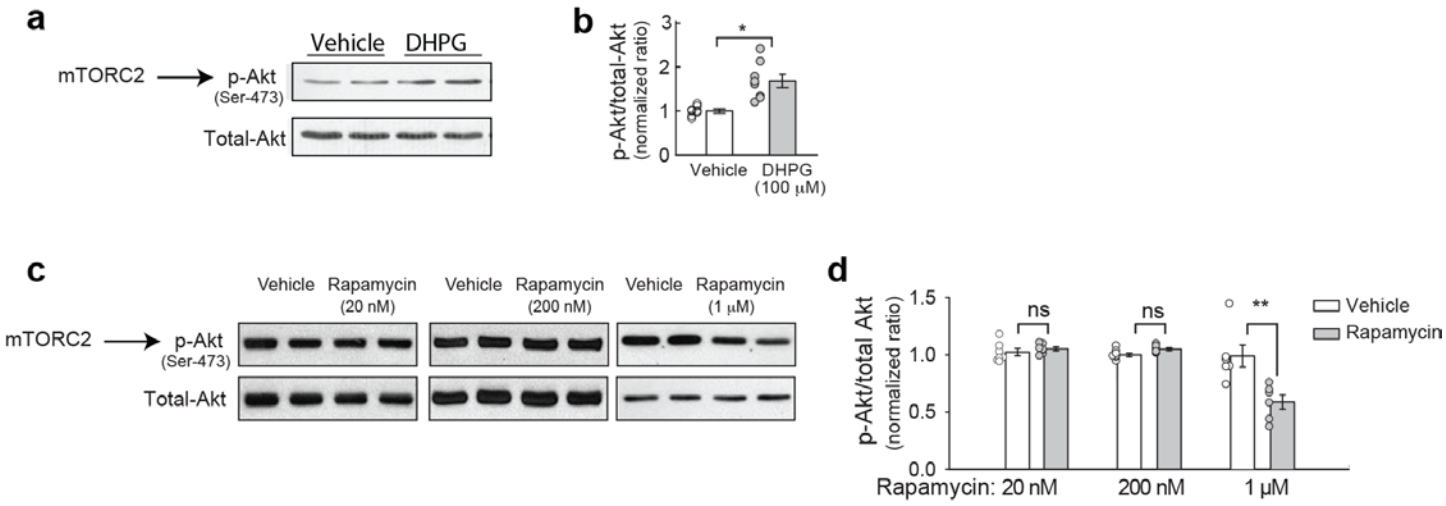


**Supplementary Figure 5**

**mTORC2 was activated by DHPG treatment and blocked by high concentration of rapamycin (1 μM)**

(**a-b**) In control hippocampal slices, DHPG (100 μM, 10 min) triggers mTORC2 activity, as determined by increased phosphorylation of Akt at Ser-473 ($n$ = 8 per group, $P < 0.001$, Mann-Whitney rank sum test). (**c-d**) In hippocampal slices, mTORC2 is sensitive to high (1 μM, n = 6 per group, $t_{10} = 3.480$, $P = 0.006$), but not low (20 nM, vehicle $n$ = 7, rapamycin n = 7, $t_{12} = 0.699$, $P = 0.498$, or 200 nM, $n$ = 7 per group, $t_{12} = 0.570$, $P = 0.579$), concentrations of rapamycin). Bar graph shows mean ± SEM of each group. The statistics were based on two-sided Student's $t$-test. Images of western blots were cropped to show only representative samples. Full-length blots can be found in supplementary Figure 8.

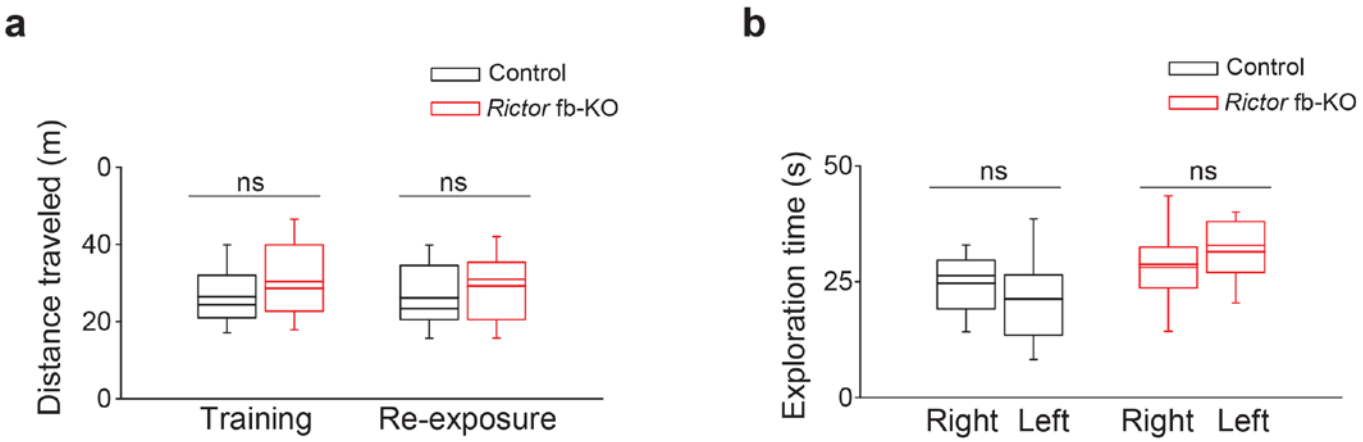


**Supplementary Figure 6**

**Normal locomotor and exploratory behavior in mTORC2-deficient mice.**

(**a-b**) Control (n = 13) and *Rictor* fb-KO mice (n = 10) travelled similar distances during spatial recognition training (**a,** $t_{21}$ = -1.307, $P$ = 0.205) and re-exposure $t_{22}$ = -0.687, $P$ = 0.449) and spent similar time exploring identical objects during object recognition training (**b**, control n = 12, Left vs. Right, $t_{22}$ = 0.988, $P$ = 0.334; *Rictor* fb-KO mice n = 11, Left vs. Right, $t_{20}$ = -0.847, $P$ = 0.407). Box plots show the minimum, maximum, median, 25$^{th}$, and 75$^{th}$ percentile of the groups. The mean values are indicated in thick lines. The statistics were based on two-sided Student's *t*-test.

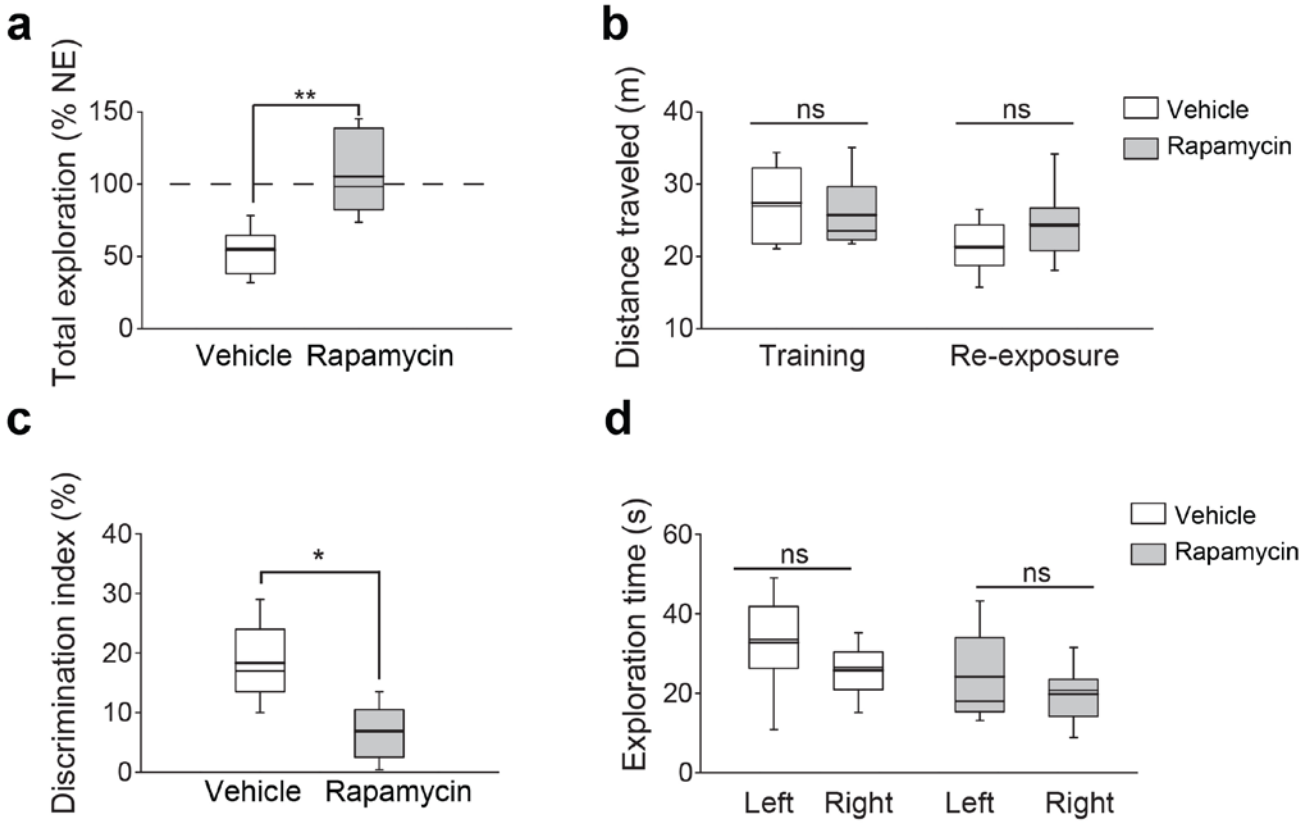


**Supplementary Figure 7**

**Rapamycin (10 mg/kg) inhibits both spatial and object place learning.**

(**a**) During re-exposure, rapamycin-treated mice (n = 10) spent significantly more time exploring the objects than vehicle-treated mice (n = 10, $t_{18}$ = -5.089, $P$ < 0.001). (**b**) Vehicle (n = 10) and rapamycin-treated (n = 10) mice travelled similar distances during spatial recognition training ($t_{18}$ = 0.760, $P$ = 0.457) and re-exposure ($t_{18}$ = -1.589, $P$ = 0.129). (**c**) Object recognition is impaired in rapamycin-treated mice (n = 9), since they show significantly less preference for novel objects compared to vehicle group (n = 9; $t_{16}$ = 4.530, $P$ < 0.001). (**d**) Rapamycin-treated and vehicle-treated mice spent similar time exploring identical objects during object recognition training (vehicle n=9, Left vs. Right $t_{16}$ = 1.167, $P$ = 0.125; Rapamycin n=9, Left vs. Right $t_{16}$ = 1.060, $P$ = 0.323). Box plots show the minimums, maximums, median, 25$^{th}$, and 75$^{th}$ percentile of the groups. The mean values are indicated in thick lines. The statistics were based on two-sided Student's *t*-test.

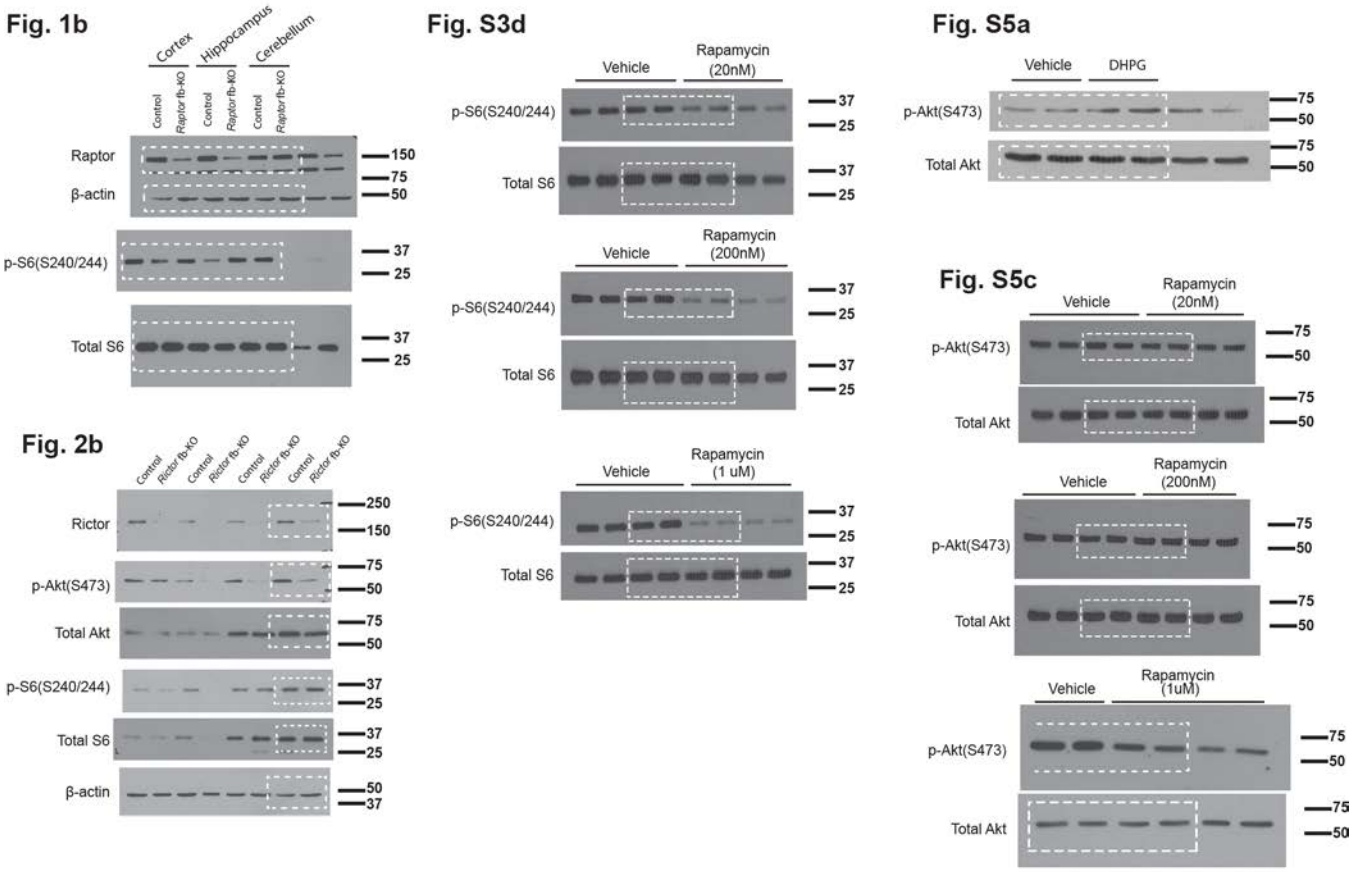


**Supplementary Figure 8**

**Images of full-length blots presented in main and supplementary figures.**